THE JOURNAL OF PHYSICAL CHEMISTRY Letters

Letter

pubs.acs.org/JPCL

STM Luminescence Spectroscopy of Intrinsic Defects in ZnO(000$\bar{1}$) Thin Films

Fernando Stavale,[†,‡] Niklas Nilius,*[,†,§] and Hans-Joachim Freund[†]

[†]Fritz-Haber-Institut der Max-Planck-Gesellschaft, Faradayweg 4-6, D-14195 Berlin, Germany

[‡]Centro Brasileiro de Pesquisas Físicas - CBPF/MCTI, Rua Dr. Xavier Sigaud 150, 22290-180 Rio de Janeiro, Brazil

[§]Institut für Physik, Carl von Ossietzky Universität Oldenburg, D-26111 Oldenburg, Germany

ABSTRACT: Luminescence spectroscopy with an STM is used to analyze the role of lattice defects in crystalline ZnO films grown on Au(111). The films exhibit a strong band-recombination peak at 373 nm as well as three maxima at higher wavelength, indicating the presence of oxide defects. To identify their nature, we systematically alter the preparation conditions by treating the films with UV radiation, hydrogen, and oxygen and at elevated temperature. From concomitant changes in the emission response, we are able to assign the subgap peaks to specific O and Zn defects in the wurtzite lattice. Our conclusions are discussed in light of recent DFT calculations.

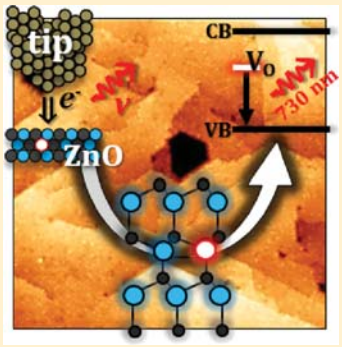

SECTION: Spectroscopy, Photochemistry, and Excited States

Zinc oxide has recently seen a boost in research activities, triggered by the relevance of the material to fabricate optoelectronic devices, gas sensors, and heterogonous catalysts, for example, for methanol synthesis.[1−3] However, key properties of the oxide are still not well understood, and the role of lattice defects and impurities is heavily debated. For example, the n-type conductivity of ZnO has long been associated with defects without realizing that hydrogen plays the role of the hidden donor.[4] Conversely, the fabrication of p-type ZnO is still an experimental challenge as classical approaches such as nitrogen doping did not yield the desired results.[5,6] Both issues highlight the role of unidentified defects that cancel the impact of the built-in dopants.

The ambiguous role of lattice defects becomes particularly evident in the optical behavior of ZnO.[7−10] Due to its direct band gap, the oxide features several strong transitions, with the band-recombination peak at 3.3 eV being the most prominent one. Additional peaks with sub-band-gap energy indicate the presence of defect-mediated emission channels, the origin of which is controversially debated in the literature.[6−11] In fact, most native ZnO defects with finite thermodynamic stability, such as Zn and O vacancies (V_{Zn}, V_O), interstitials (Zn_i, O_i), and antisite defects, have been proposed as potential emission centers. In addition, various impurity ions, in particular, nitrogen, were linked to common ZnO emission bands. The difficulty to connect luminescence data to lattice defects arises from the strong dependence of defect concentrations on the different ZnO preparation conditions, in particular, the Zn/O chemical potential. Moreover, the oxide defects have a large tendency to interact and compensate each other. Given the variety of fabrication methods, it is therefore not very surprising that different ZnO samples feature different defect landscapes and hence different optical properties.

At present, the most reliable information on ZnO defects comes from theoretical studies that accurately predict ground-state properties (e.g., defect formation energies) but are less reliable when it comes to the excited states and the optical response.[12,13] Luminescence experiments on well-characterized ZnO samples are therefore desirable to confirm the theoretical predictions. In this study, we aim to fulfill this requirement by growing crystalline ZnO films on Au(111) supports and by measuring local luminescence data with an STM.[14] In order to elucidate the nature of defects, we have prepared nearly stoichiometric films as well as films with varying concentrations of ZnO point defects. From differences in the optical response, we draw conclusions on the interrelation of native ZnO defects and characteristic maxima in the photon emission spectra. In particular, we demonstrate that the 730 nm emission peak is not related to nitrogen, as proposed before but relates to V_O defects in the lattice.[15,16]

Figure 1 displays an STM image and the corresponding differential conductance spectrum of a well-prepared ZnO film. The entire surface is covered by Å-sized protrusions, being assigned to hydrogen species that cancel the intrinsic polarity of O-terminated ZnO (000$\bar{1}$).[17,18] The dI/dV spectrum reveals the common n-type character of ZnO as the conduction band onset at 0.9 V is much closer to the Fermi level than the valence

Received: August 27, 2013
Accepted: November 6, 2013
Published: November 6, 2013

   dx.doi.org/10.1021/jz401823c | *J. Phys. Chem. Lett.* 2013, 4, 3972−3976

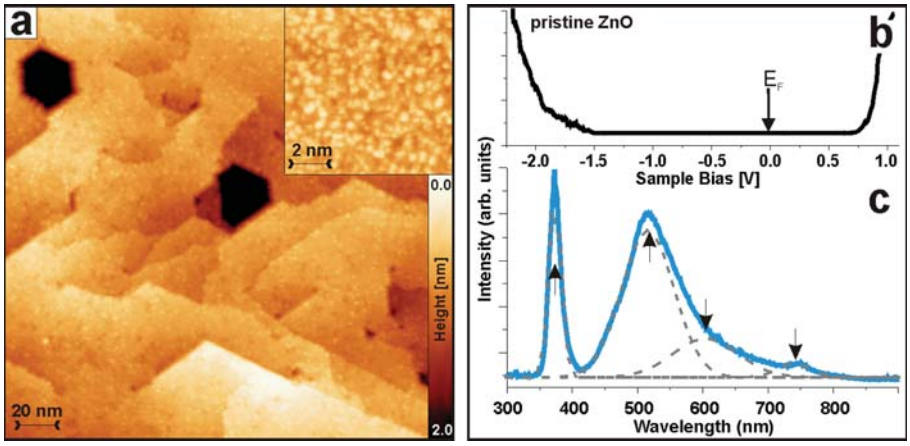

Figure 1. (a) Overview and high resolution STM image of 25 ML ZnO grown on Au(111) (1 nA, 3.4 V, 220 × 220 nm^2). (b) Corresponding dI/dV spectrum taken with the lock-in technique and a 0.7 V set point bias. Note the n-type conductance behavior. (c) Luminescence spectra of 25 ML ZnO. Respective emission maxima have been determined via Gaussian deconvolution (see arrows).

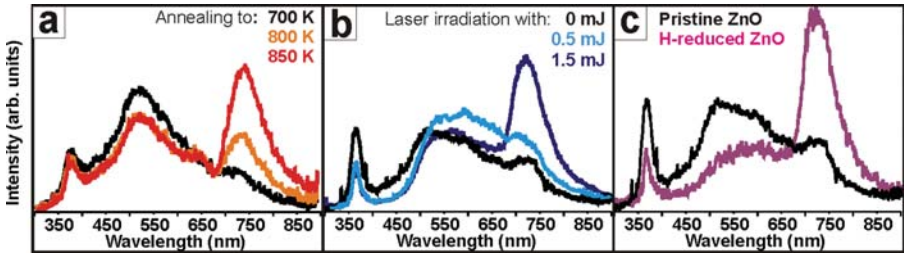

Figure 2. Luminescence spectra of pristine and reduced ZnO films. (a) Thermal treatment in 2 × 10^{-5} mbar of O_2 at 700 K (black) and in vacuum at 800 (orange) and 850 K (red). (b) Reduction with 3.5 eV photons: pristine film (black), after exposure to 0.5 (light blue) and 1.5 mJ/cm^2 laser fluence (dark blue). (c) Chemical reduction: pristine film (black) and film grown in atomic hydrogen (violet).

band at −2.1 V. The total gap width of 3.0 V is slightly smaller than the bulk value of 3.3 V. Although no gap states are detected in the dI/dV curve, the film is not perfect as several emission peaks become visible in STM luminescence spectra (Figure 1c). The first one is centered at 373 nm (3.3 eV) and has a fwhm of 160 meV. It is readily assigned to the band-recombination in ZnO as the dominant transition in defect-poor materials. The band transition is mediated by excitons, that is, free or defect-bound electron−hole pairs, and actually gives rise to a series of emission lines with energies just below the fundamental gap value.[19] Due to the relatively high acquisition temperature of 100 K, the excitonic fine structure is not resolved in our case. We note that the band recombination occurs primarily in the interior of the film, and the emission response hardly changes upon covering the surface with gold. This finding is in contrast to earlier studies on MgO, where most of the recombination centers were found at the surface and could be passivated via gold exposure.[20] Besides the fundamental ZnO emission, three peaks with subgap energies are detected in the luminescence spectra (Figure 1c). The first two at 535 (2.3 eV) and 595 nm (2.1 eV) are relatively broad (250 meV fwhm), while the last one at 730 nm (1.7 eV) has only ∼90 meV fwhm. In order to identify the underlying emission centers, we have altered the abundance of native ZnO defects and monitored the associated changes in the optical response, as discussed next.

In a first step, we have prepared ZnO films at reducing conditions in order to insert O vacancies into the lattice. Oxide reduction was achieved either by thermal,[21] optical,[22,23] or chemical means.[24,25] Figure 2a shows the evolution of the ZnO luminescence upon vacuum annealing. The main spectral change concerns the 730 nm peak that intensifies by nearly a factor of 5, whereas other maxima remain unchanged. As vacuum annealing affects also the abundance of Zn defects, we have chosen an optical route to reduce the oxide as a next step. For this purpose, the samples were exposed in situ to UV photons of 3.5 eV energy, using the third harmonic of a Nd:YAG laser. The laser fluence was varied between 0.5 and 1.5 mJ/cm^2, sufficiently small to suppress thermal effects. Also in this experiment, mainly the 730 nm peak gained intensity, while other lines remained constant (Figure 2b). Finally, chemical reduction was realized by exposing the films to atomic hydrogen during growth, followed by an annealing step at 600 K (Figure 2c). Hydrogen is known to interact with lattice oxygen and leads to the formation of water that leaves the surface at elevated temperature.[22] Mainly the 730 nm peak pops up again, demonstrating that all reduction pathways affect the same optical transition that is likely related to V_O defects in the lattice, as shown below.

Another defect type, oxygen interstitials (O_i), was produced by implanting O ions into the as-grown ZnO film at room temperature. The lattice quality was restored afterward by annealing the oxide to 600 K in 2 × 10^{-5} mbar of oxygen. Luminescence spectra of such samples lacked the 730 nm emission peak that was typical for the reduced oxide. In contrast, an intensity gain was found for the 595 nm peak, smaller than that for the 730 nm emission observed upon reduction (Figure 3a). In a final experiment, we focused on Zn

dx.doi.org/10.1021/jz401823c | J. Phys. Chem. Lett. 2013, 4, 3972−3976

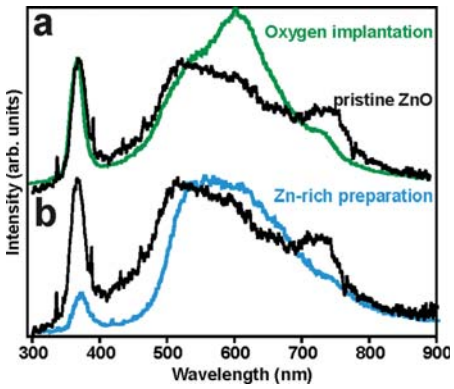

Figure 3. Luminescence spectra of pristine ZnO (black) and films grown in the presence of atomic oxygen (green) and excess Zn (blue).

defects. Their abundance turned out to be difficult to change as V_{Zn} defects play an important role in compensating for the excess electrons in n-type ZnO.[12] In principle, the V_{Zn} concentration can only be decreased if all preparation steps are performed at finite Zn chemical potential, which is however a challenging task in an UHV experiment. To tackle the problem, we have prepared Zn-rich films by exposing the Au(111) support simultaneously to ZnO vapor and metallic Zn from a second source, followed by an annealing step at 600 K in 5×10^{-8} mbar of O_2. The optical response of these films featured a substantial reduction of the 535 nm emission, while other peaks were less affected by the Zn excess (Figure 3b). This finding suggests that Zn-related defects might be responsible for luminescence in the green spectral range. On the basis of our experimental results, we propose the following correlation between ZnO emission maxima and native defects in the wurtzite lattice.

Oxygen Vacancies (V_O). According to the DFT phase diagram,[12] V_O defects are thermodynamically less stable than Zn vacancies in n-type ZnO. Consequently, optical transitions mediated by O defects should be weak in well-prepared films, a requirement that is only met by the 730 nm peak (Figure 1c). Moreover, this peak gains intensity upon reducing the films by thermal, optical, or chemical means, a process that is known to introduce V_O defects into the lattice (Figure 2). According to recent DFT calculations, these defects produce gap states that will be doubly occupied in our films due to the high Fermi level and the presence of the Au(111) electron reservoir beneath.[12] Two pathways may now account for the peak in the electron-stimulated photon emission, (i) hole formation in the ZnO valence band followed by radiative decay of electrons from the V_O gap states or (ii) hole formation in the V_O gap states and recombination with conduction band electrons. In both cases, the V_O defect level needs to be located in the middle of the band gap in order to produce an emission peak at 730 nm. The two mechanisms have been proposed before, for example, for the interpretation of optically detected EPR data;[7] however, only the first scenario could be reproduced in DFT calculations.[12,13] Also, luminescence data obtained on ZnO samples bombarded by MeV electrons supported the concept of hole-capturing by doubly charged V_O defects.[10,26] Following these arguments, we assign the luminescence at 730 nm to O vacancies and challenge earlier interpretations that relate the red emission to nitrogen impurities in the ZnO lattice.[15,16]

Zinc Vacancies (V_{Zn}). The role of Zn vacancies in luminescence spectra is more difficult to evaluate as their concentration is hard to adjust experimentally. We suggest a correlation between Zn defects and the 535 nm emission for the following reasons. First, the 535 nm peak has the highest intensity of all subgap maxima and cannot be quenched entirely with our preparation methods. This agrees well with the low formation energy of V_{Zn} in theoretical approaches, being rationalized by the need to insert this defect to reach charge balance with the excess electrons in the conduction band of n-type ZnO.[12] Only when E_F is close to the valence band, a situation that is not met experimentally, do V_O defects become energetically preferred. Second, oxide preparation in an excess of metallic Zn causes the 535 nm peak to decrease, which points to a partial annihilation of the V_{Zn} defects (Figure 3b). However, the number of Zn vacancies cannot be put to zero as new defects develop spontaneously in the lattice upon annealing the film. Still, our arguments support a correlation between V_{Zn} defects and the 535 nm emission peak.

In a mechanistic picture, the Zn vacancies introduce acceptor-type gap states close to the valence band that will fill up with electrons at the high Fermi level in our films (V_{Zn}^{2-} centers).[12] The defects become optically active if holes are generated in the respective states, either directly via ionization by the incoming tip electrons or indirectly via capturing a hole from the valence band (Figure 4). In both cases, the excited

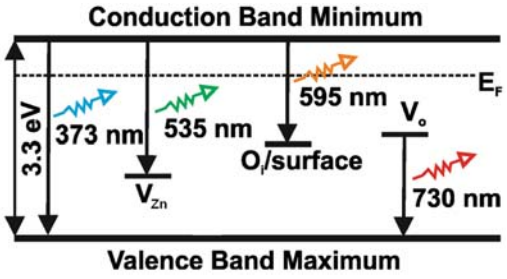

Figure 4. ZnO band diagram with the approximate positions of defect levels as deduced from the optical data.

V_{Zn}^- center can recombine with a hot electron in the conduction band, producing the 535 nm emission line. From the wavelength difference to the V_O emission at 730 nm, we position the V_{Zn}^- gap state ~0.6 eV closer to the valence band than the V_O state. This conclusion is in line with DFT calculations that find an energy difference of 0.9 eV between the V_{Zn}^{2-}/V_{Zn}^- and the V_O^0/V_O^+ transition states, a value that ignores however relaxation effects in the system during the optical transition.[11] We note that an assignment of the 535 nm peak is in agreement with earlier studies on ZnO single crystals and powders,[8,9] although no unambiguous interpretation has been reached so far.

Other Defects. The interpretation of the 595 nm peak in the ZnO luminescence is least settled. The peak occurs already in the as-grown films, indicating that the associated defect has low formation energy and spontaneously develops at our growth conditions. Consulting DFT stability diagrams for n-doped ZnO,[12,13] we find that O interstitials are the most stable defects after the V_{Zn} at the O-rich conditions used in our work. The defects occur in two configurations, either as an additional O^{2-} ion in an octahedral lattice site or as quasi-molecular species occupying the original anion position. Whereas the latter is optically inactive, the former induces an acceptor state in the lower part of the gap that gets filled up with electrons in our

dx.doi.org/10.1021/jz401823c | J. Phys. Chem. Lett. 2013, 4, 3972−3976

films. Upon ionization via electrons from the tip, a radiative recombination channel opens up for conduction-band electrons, similar to the scenario proposed for V_{Zn}. Taking the emission peak at 595 nm as a fingerprint for this transition, we may estimate the energy position of the ionized O_i state to be at 1.2 eV above the valence band edge (Figure 4). This value compares to calculated transition levels for singly and doubly charged O_i defects at 0.7 and 1.5 eV, respectively.[12] Apart from such an energetic match, the 595 nm peak is most sensitive to the growth of ZnO in the presence of atomic oxygen, being a potential source for O interstitials in the lattice (Figure 3a).

We note that the 595 nm emission is frequently observed also in ZnO nanostructures, for example, rods, tubes, and coils.[27,28] This opens an alternative explanation for the peak as due to recombination of ZnO excitons at distinct surface sites. It is well established that the oxide gap narrows down at the surface, either due to a reduced Madelung potential or specific surface states.[29] As surface contributions are naturally strong in thin films, we expect that a corresponding peak might be visible, although no comparable emission is reported for bulk crystals.

In conclusion, STM luminescence spectra of flat ZnO films prepared on Au(111) single crystals exhibit not only the common band recombination peak but also several defect-related emission lines. By systematically varying the preparation conditions, we have identified likely candidates for the underlying lattice defects. Our study demonstrates how thin-film techniques in combination with optical approaches can be used to elucidate the defect landscape in oxide materials, being of fundamental importance for their physical and chemical properties.

EXPERIMENTAL METHODS

All measurements were performed in an ultrahigh vacuum, liquid-nitrogen-cooled STM setup, specifically designed to detect photons from the tip−sample junction.[30] For this purpose, a Beetle-type STM head is placed inside of a parabolic mirror, which collects photons from the tip−sample junction and directs them to a grating spectrograph (500 nm blazing) coupled to a CCD detector. Luminescence spectra were obtained by retracting the tip from the tunnel junction and adjusting a 5 nA emission current at a 150 V bias voltage with the STM feedback. The outgoing radiation was accumulated for 300 s, so that even small photon fluxes could be detected with 100 nm spatial resolution. Oxide films of 25 ML thickness were prepared by sublimating high-purity ZnO pellets via e-beam heating in an O_2 ambience of 2×10^{-5} mbar and depositing the vapor onto a Au(111) surface at 300 K.[17] Subsequent annealing in O_2 transformed the amorphous oxide into a crystalline film, which displayed the characteristic hexagonal (1×1) LEED pattern of wurtzite ZnO$(000\bar{1})$. The film quality was confirmed with STM topographic images that showed wide, atomically flat terraces delimited by straight step edges (Figure 1a). To alter the ZnO defect structure, the films were annealed to temperatures between 650 and 850 K and exposed to atomic hydrogen or oxygen. The respective species, produced by an ion gun, have been inserted into the surface with 250 eV kinetic energy; possible defects were removed afterward by gentle oxygen annealing.

AUTHOR INFORMATION

Corresponding Author

*E-mail: nilius@fhi-berlin.mpg.de.

Notes

The authors declare no competing financial interest.

ACKNOWLEDGMENTS

F.S. thanks the Alexander v. Humboldt Stiftung for financial support. The authors acknowledge support from the DFG Cluster of Excellence "UniCat".

REFERENCES

(1) Wöll, C. The Chemistry and Physics of Zinc Oxide Surfaces. *Prog. Surf. Sci.* **2007**, *82*, 55−120.
(2) Oba, F.; Choi, M.; Togo, A.; Tanaka, I. Point Defects in ZnO: An Approach from First Principles. *Sci. Technol. Adv. Mater.* **2011**, *12*, 034302.
(3) Dulub, O.; Boatner, L. A.; Diebold, U. STM Study of the Geometric and Electronic Structure of ZnO(0001)-Zn. *Surf. Sci.* **2002**, *519*, 201−217.
(4) Du, M. H.; Biswas, K. Anionic and Hidden Hydrogen in ZnO. *Phys. Rev. Lett.* **2011**, *106*, 115502.
(5) Hapiuk, D.; Marques, M. A. L.; Melinon, P.; Flores-Livas, J. A.; Botti, S.; Masenelli, B. p-Doping in Expanded Phases of ZnO: An Ab Initio Study. *Phys. Rev. Lett.* **2012**, *108*, 115903.
(6) Look, D. C.; Farlow, G. C.; Reunchan, P.; Limpijumnong, S.; Zhang, S. B.; Nordlund, K. Evidence for Native-Defect Donors in n-Type ZnO. *Phys. Rev. Lett.* **2005**, *95*, 225502.
(7) Vlasenko, L. S.; Watkins, G. D. Optical Detection of Electron Paramagnetic Resonance in Room-Temperature Electron-Irradiated ZnO. *Phys. Rev. B* **2005**, *71*, 125210.
(8) Selim, F. A.; Weber, M. H.; Solodovnikov, D.; Lynn, K. G. Nature of Native Defects in ZnO. *Phys. Rev. Lett.* **2007**, *99*, 085502.
(9) Ton-That, C.; Weston, L.; Phillips, M. R. Characteristics of Point Defects in the Green Luminescence from Zn- and O-Rich ZnO. *Phys. Rev. B* **2012**, *86*, 115205.
(10) Knutsen, K. E.; Galeckas, A.; Zubiaga, A.; Tuomisto, F.; Farlow, G. C.; Svensson, B. G.; Kuznetsov, A. Y. Zinc Vacancy and Oxygen Interstitial in ZnO Revealed by Sequential Annealing and Electron Irradiation. *Phys. Rev. B* **2012**, *86*, 121203.
(11) Tanaka, S.; Takahashi, K.; Sekiguchi, T.; Sumino, K.; Tanaka, J. Cathodoluminescence from Fractured Surfaces of ZnO Varistors. *J. Appl. Phys.* **1995**, *77*, 4021−4023.
(12) Janotti, A.; Van de Walle, C. G. Native Point Defects in ZnO. *Phys. Rev. B* **2007**, *76*, 165202.
(13) Janotti, A.; Van de Walle, C. G. Oxygen Vacancies in ZnO. *Appl. Phys. Lett.* **2005**, *87*, 122102.
(14) Likovich, E. M.; Jaramillo, R.; Russell, K. J.; Ramanathan, S.; Narayanamurti, V. Narrow Band Defect Luminescence from Al-Doped ZnO Probed by Scanning Tunneling Cathodoluminescence. *Appl. Phys. Lett.* **2011**, *99*, 151910.
(15) Tarun, M. C.; Zafar Iqbal, M.; McCluskey, M. D. Nitrogen is a Deep Acceptor in ZnO. *AIP Adv.* **2011**, *1*, 022105.
(16) Lyons, J. L.; Janotti, A.; Van de Walle, C. G. Why Nitrogen Cannot Lead to *p*-Type Conductivity in ZnO. *Appl. Phys. Lett.* **2009**, *95*, 252105.
(17) Stavale, F.; Pascua, L.; Nilius, N.; Freund, H.-J. Morphology and Luminescence of ZnO Films Grown on a Au(111) Support. *J. Phys. Chem. C* **2013**, *117*, 10552−10557.
(18) Lauritsen, J. V.; Porsgaard, S.; Rasmussen, M. K.; Jensen, M. C. R.; Bechstein, R.; Meinander, K.; Clausen, B. S.; Helveg, S.; Wahl, R.; Kresse, G.; Besenbacher, F. Stabilization Principles for Polar Surfaces of ZnO. *ACS Nano* **2011**, *5*, 5987−5994.
(19) Meyer, B. K.; Alves, H.; Hofmann, D. M.; Kriegseis, W.; Forster, D.; Bertram, F.; Christen, J.; Hoffmann, A.; Strassburg, M.; Dworzak, M.; Haboeck, U.; Rodina, A. V. Bound Exciton and Donor−Acceptor Pair Recombinations in ZnO. *Phys. Status Solidi B* **2004**, *241*, 231−260.
(20) Benia, H. M.; Lin, X.; Gao, H.-J.; Nilius, N.; Freund, H.-J. Nucleation and Growth of Gold on MgO Thin Films: A Combined

STM and Luminescence Study. *J. Phys. Chem. C* **2007**, *111*, 10528−10533.
(21) Dupuis, A.-C.; Abu-Haija, M.; Richter, B.; Kuhlenbeck, H.; Freund, H.-J. V_2O_3(0001) on Au(111) and W(110): Growth, Termination and Electronic Structure. *Surf. Sci.* **2003**, *539*, 99−112.
(22) Trevisanutto, P. E.; Sushko, P. V.; Shluger, A. L.; Beck, K. M.; Henyk, M.; Joly, A. G.; Hess, W. P. A Mechanism of Photo-Induced Desorption of Oxygen Atoms from MgO Nano-Crystals. *Surf. Sci.* **2005**, *593*, 210−220.
(23) Sterrer, M.; Diwald, O.; Knozinger, E.; Sushko, P. V.; Shluger, A. L. Energies and Dynamics of Photoinduced Electron and Hole Processes on MgO Powders. *J. Phys. Chem. B* **2002**, *106*, 12478−12482.
(24) Berger, T.; Sterrer, M.; Diwald, O.; Knözinger, E. The Color of the MgO Surface—A UV/Vis Diffuse Reflectance Investigation of Electron Traps. *J. Phys. Chem. B* **2004**, *108*, 7280−7285.
(25) Knudsen, J.; Merte, L. R.; Grabow, L. C.; Eichhorn, F. M.; Porsgaard, S.; Zeuthen, H.; Vang, R. T.; Lægsgaard, E.; Mavrikakis, M.; Besenbacher, F. Reduction of FeO/Pt(111) Thin Films by Exposure to Atomic Hydrogen. *Surf. Sci.* **2010**, *604*, 11−20.
(26) Evans, S. M.; Giles, N. C.; Halliburton, L. E.; Kappers, L. A. Further Characterization of Oxygen and Zinc Vacancies in Electron-Irradiated ZnO. *J. Appl. Phys.* **2008**, *103*, 043710.
(27) Shalish, I.; Temkin, H.; Narayanamurti, V. Size-Dependent Surface Luminescence in ZnO Nanowires. *Phy. Rev. B* **2004**, *69*, 245401.
(28) Lin, X.; He, X. B.; Yang, T. Z.; Guo, W.; Shi, D. X.; Gao, H.-J.; Ma, D. D.; Lee, S. T.; Liu, F.; Xie, X. C. Intrinsic Current−Voltage Properties of Nanowires with Four-Probe Scanning Tunneling Microscopy: A Conductance Transition of ZnO Nanowire. *Appl. Phys. Lett.* **2006**, *89*, 043103.
(29) Sushko, P. V.; Shluger, A. L. Electronic Structure of Excited States at Low-Coordinated Surface Sites of MgO. *Surf. Sci.* **1999**, *421*, L157−L176.
(30) Freund, H.-J.; Nilius, N.; Risse, T.; Schauermann, S.; Schmidt, T. Innovative Measurement Techniques in Surface Science. *ChemPhysChem* **2011**, *12*, 79−87.